agronomy

MDPI

Article

Energetic Constraints and Carbon Efficiency During Sucrose Storage in Sugarcane Culms

Frederik C. Botha [1,2]

[1] Queensland Alliance for Agriculture and Food Innovation (QAAFI), University of Queensland, St. Lucia, QLD 4072, Australia; f.botha@uq.edu.au
[2] ARC Research Hub for Engineering Plants to Replace Fossil Carbon, University of Queensland, St. Lucia, QLD 4072, Australia

Abstract

Sugarcane stores sucrose in a living culm for extended periods, yet the respiratory cost of maintaining this storage tissue remains poorly quantified. We quantified growth and maintenance respiration along the culm (internodes 1 to 12) in three genotypes at mid-season (rapid growth) and end-season (maturation) using a composition-based carbon accounting framework derived from measurements of biomass accumulation and composition. Growth respiration was highest in elongating internodes (3 to 6) and declined with maturation, whereas maintenance respiration increased progressively and dominated in mature storage internodes (10 to 12). Consequently, total sink demand remained substantial even after structural growth slowed, indicating that mature internodes continue to require significant metabolic input despite limited biomass production. To evaluate the potential impact of energetic constraints, we simulated reduced mitochondrial energy contribution to assess the sensitivity of respiratory carbon demand to decreased energetic efficiency. These simulations predicted an increase in glucose requirement for respiration across all internodes, with the largest proportional effect in mature tissue where maintenance costs dominated. Despite this predicted increase in respiratory demand, sucrose accumulation was maintained in mature culms, indicating that respiratory carbon loss remains constrained during storage. This suggests that storage tissue operates with relatively high carbon-use efficiency during maintenance-dominated metabolism. We interpret this pattern as consistent with metabolic configurations that reduce ATP demand, potentially involving partial substitution of ATP-dependent reactions by pyrophosphate (PPi)-dependent pathways, although this mechanism was not directly measured. These findings highlight the importance of maintenance respiration and energetic efficiency in determining sink strength and sucrose yield, and they provide a physiological framework for understanding carbon conservation in long-lived storage organs.

Keywords: respiration; pyrophosphate; hypoxia; sucrose accumulation

Check for updates

Academic Editor: Guanfu Fu

Received: 15 March 2026
Revised: 23 April 2026
Accepted: 28 April 2026
Published: 30 April 2026

Copyright: © 2026 by the author. Licensee MDPI, Basel, Switzerland. This article is an open access article distributed under the terms and conditions of the Creative Commons Attribution (CC BY) license.

1. Introduction

Sugarcane (*Saccharum* spp.) is one of the most productive C_4 crops and accumulates large quantities of sucrose in the stem rather than in reproductive organs. Mature culms commonly contain 15–20% sucrose on a fresh-weight basis while the tissue remains alive and hydrated [1]. Unlike seeds or storage roots that undergo metabolic quiescence, sugarcane stores carbohydrates in living parenchyma cells for several months. Consequently, the culm remains an active metabolic sink throughout its lifespan.

In plant carbon balance theory, assimilated carbon is partitioned between structural growth, respiration, and storage [2–5]. During early internode development, respiratory demand is dominated by biosynthesis, but, as elongation slows, maintenance processes become the primary metabolic cost. Continued sucrose accumulation during maturation therefore implies that phloem import exceeds respiratory carbon loss even when growth declines. The physiological question is not whether sucrose is respired but whether the carbon cost of maintaining living storage tissue is sufficiently low to permit sustained net accumulation.

An additional constraint on culm metabolism is internal oxygen supply. Oxygen diffusion in water-saturated tissues is slow, and bulky plant organs commonly develop internal oxygen gradients [6–8]. Hypoxic conditions have been demonstrated in storage tissues such as potato tubers [9] and developing seeds [10,11], where restricted oxygen availability alters respiratory metabolism and cellular energy balance. The sugarcane culm has similar anatomical features, with vascular bundles separated from storage parenchyma by multiple cell layers [1], implying that sucrose accumulation likely occurs under chronically reduced oxygen availability.

Reduced oxygen availability limits oxidative phosphorylation and decreases the efficiency of ATP generation [6]. Under energetic constraint, more substrate may be required to satisfy a given ATP demand. In a living storage organ where maintenance respiration dominates during maturation, such a decrease in energetic efficiency would increase the carbon cost of maintaining sink activity. The critical issue is therefore not whether sucrose is respired but whether the energetic cost of maintenance metabolism remains compatible with sustained net sucrose import and accumulation.

Plants experiencing energetic limitation can adjust metabolism to reduce ATP demand while maintaining metabolic flux [12]. One mechanism is the utilisation of inorganic pyrophosphate (PPi) as an alternative phosphoryl donor [13]. PPi-dependent reactions can partially substitute for ATP-requiring steps in glycolysis and sucrose cycling, thereby lowering ATP demand and reducing the respiratory substrate required to support maintenance metabolism [12,14–16]. In an oxygen-limited storage tissue, such a metabolic configuration would allow the culm to remain an active sink while limiting the carbon cost of maintenance respiration.

The objective of this study was to quantify the developmental shift from growth-dominated to maintenance-dominated respiration along the sugarcane culm and to determine how energetic constraint alters the carbon cost of maintaining storage tissue. Using a composition-based carbon accounting framework, we estimated growth and maintenance respiration across internodes representing active elongation and mature storage. We then evaluated the sensitivity of respiratory carbon demand to reduced mitochondrial energy contribution to assess whether sustained sucrose accumulation can be reconciled with maintenance-dominated metabolism under oxygen limitation.

It is important to note that internal oxygen concentrations within the culm were not directly measured in this study. Instead, we used a composition-based carbon accounting framework combined with simulation to assess the sensitivity of respiratory carbon demand to reduced energetic efficiency associated with oxygen limitation. This approach allowed evaluation of the physiological consequences of internal oxygen gradients without disturbing the in situ metabolic state of the tissue. We hypothesised that maintenance-dominated metabolism in mature sugarcane internodes operates under energetic constraint, increasing the potential carbon cost of respiration, but that this cost is moderated by metabolic configurations that reduce ATP demand.

2. Materials and Methods

2.1. Plant Material, Staging, and Sampling

The growth of three sugarcane varieties, KQ228, Q240, and SRA3, was monitored over a plant and ratoon crop. The trial was established at the Salvetti Farming Company, Farm 6207 (17°06′08″ S, 145°20′28″ E). The experiment was planted in a completely randomised design with three replicate plots per treatment, each consisting of four 10 m rows of cane. Billets obtained from disease-free stalks were used as planting material. The trial site was fully irrigated. Daily maximum and minimum air temperatures for the entire cropping cycle were obtained from the SILO database (https://www.longpaddock.qld.gov.au/silo/point-data/#responseTab2s, accessed on 1 January 2026) [17]. Thermal time, expressed as growing degree days (GDDs) for phyllochron production, was calculated as previously described using a base temperature of 10 °C [18].

2.2. Non-Destructive Sampling

Eight primary shoots in each plot were tagged for easy identification. Stalk elongation and phyllochron development were non-destructively measured in the field. This was done to ensure minimal disruption to canopy development by not changing shoot and leaf numbers, leaf production rates, or numbers of senescing leaves. Measurements were conducted on a two-weekly basis throughout the first six months of crop development and thereafter on a monthly basis.

2.3. Destructive Sampling

Eight culm samples were collected from the field plots approximately 6 and 12 months after planting. The culm samples were disintegrated using either a garden mulcher or Dedini laboratory disintegrator at room temperature. The mulched material was then weighed to determine the fresh weight (FW) and transferred to a paper bag to be dried at 70 °C until a constant dry weight (DW) was reached (usually after 4 to 5 days).

2.4. Lipids and Ion-Exchange Fractionation of Water-Soluble Constituents

Lipids were extracted from dried tissue (5.0 g) using methanol:chloroform:water (12:5:3, *v*/*v*/*v*) as described by Dickson [19]. Samples were centrifuged (4000× *g*, 10 min), and the supernatant was collected. Phase separation was induced by the addition of chloroform (5 mL) and deionised water (4 mL). The chloroform phase was recovered, dried under vacuum, and weighed to determine lipid content.

The aqueous phase was dried by rotary evaporation (40–50 °C) and re-dissolved in 70% (*v*/*v*) ethanol prepared with HPLC-grade water. Water-soluble constituents were fractionated by ion-exchange chromatography using Dowex 50W-X8 (H^+ form; 5 mL bed volume) and Dowex 1-X8 (formate form; 5 mL bed volume) columns in tandem, with the cation-exchange column positioned upstream of the anion-exchange column [19]. The ion exchange resins were obtained form ThermoFisher Scientific Australia Pty Ltd., Brisbane, Australia. Following sample application, the columns were separated, and each column was washed individually prior to elution. Compounds retained on Dowex 50W-X8 (cationic fraction) were eluted with four column volumes of 4 M NH_4OH, and compounds retained on Dowex 1-X8 (anionic fraction) were eluted with four column volumes of 4 M formate. The formate eluate was dried by rotary evaporation (40–50 °C), and the residue was weighed as the soluble organic acid fraction. Recovery and fractionation performance were verified routinely using mixed standards, confirming effective binding to each resin and quantitative elution under the conditions described.

Total amino acids in the NH_4OH eluate were estimated using a ninhydrin assay [20]. Fresh ninhydrin reagent was prepared immediately before use [20]. Samples and reagent

were mixed (1:1, v/v), heated in a boiling water bath (10 min), and cooled on ice. Ethanol (50%, v/v) was added (2.5 volumes) and mixed thoroughly, and absorbance was recorded at 570 nm. Aspartic acid was used as a standard (0–50 $\mu g\,mL^{-1}$).

2.5. Biomass Compositional Analysis

Biomass compositional analyses were performed by Celignis Analytical (Limerick, Ireland) using the P19 Deluxe package. This package integrates exhaustive water and 95% ethanol extraction of biomass, followed by two-step acid hydrolysis of the extractive-free residue, thereby ensuring that structural carbohydrate values was not inflated by soluble sugars. Lignin was determined as both acid-insoluble (Klason) and acid-soluble fractions according to NREL-style protocols. Water- and ethanol-soluble sugars, as well as polyols, were quantified directly from the solvent extracts as part of the P19 suite, avoiding double counting between extractives and structural polysaccharide pools. Protein in the lignocellulosic fraction was calculated from elemental nitrogen, and ash was also reported.

2.6. Respiration Accounting and Statistical Analysis

Internode-scale growth and maintenance respiration were estimated using a composition-based carbon accounting framework driven by observed changes in dry mass and biomass composition along the culm. Briefly, for each genotype, phenotype (mid-season and end-season), and replicate, internode trajectories were ordered by internode position and analysed over successive internode intervals. Changes in compound-class pools (carbohydrate, protein, lipid, lignin, and organic acids) were converted to glucose-equivalent carbon skeleton requirements using measured composition and published carbon fractions. Growth respiration was estimated from biosynthetic construction costs associated with positive increases in compound-class pools, and maintenance respiration was inferred as the residual energetic demand required to sustain living tissue once growth-associated demand was accounted for.

To examine the energetic consequences of oxygen limitation, we simulated scenarios in which only a specified fraction of energetic demand was satisfied by mitochondrial oxidative metabolism, with the remainder met by less efficient pathways, thereby increasing the glucose requirement per unit ATP demand. These simulations were used to quantify the sensitivity of respiratory glucose demand and total sink demand to reduced oxygen availability.

Full notation, equations, parameter values, and oxygen limitation sensitivity analyses are provided in the Supplementary Methods (Sections S1–S3).

Measured Versus Derived Variables

Biomass accumulation, composition, and developmental parameters were directly measured. In contrast, growth respiration (R_g), maintenance respiration (R_m), and total sink demand (S) were derived from these measurements using the carbon accounting framework described above. These variables therefore represent model-based estimates rather than direct measurements of CO_2 exchange (e.g., using infrared gas analysis).

Composition-based respiration accounting has been widely used in plant carbon balance studies to partition growth and maintenance costs where direct measurement is not feasible [2,3,5]. While absolute values depend on parameter assumptions, the framework is robust for evaluating relative differences across developmental stages and simulated conditions.

The oxygen limitation scenarios represent sensitivity analyses in which the contribution of mitochondrial oxidative phosphorylation to ATP production is reduced. These simulations do not quantify in situ oxygen concentration but rather evaluate how reduced energetic efficiency would influence respiratory carbon demand. The assumed reduction in

mitochondrial ATP contribution was explored across a defined range (see Supplementary Methods), allowing evaluation of sensitivity rather than reliance on a single fixed parameter.

2.7. Statistical Analysis and Data Visualisation

For each phenotype and internode position, replicate measurements are summarised using the median and associated uncertainty estimated by non-parametric bootstrap confidence intervals (95%, 2000 resamples). The median was used because several variables showed non-normal distributions and unequal variances among internodes. To evaluate the metabolic effect of oxygen limitation, paired comparisons were performed between hypoxia and hypoxia + PP_i scenarios. Differences were tested using the Wilcoxon signed-rank test, with a sign test applied when sample size or tied values prevented reliable Wilcoxon estimation. Genotypic effects were analysed separately for each phenotype and internode position using a one-way analysis of variance (ANOVA). Post hoc comparisons were performed with Tukey's honestly significant difference (HSD) test, and the resulting *p*-values were adjusted for multiple testing using the Benjamini–Hochberg procedure. Effect sizes are reported as η^2. Graphical summaries were designed to illustrate the energetic balance of respiration. Energy supply was partitioned into aerobic ATP production (ATP_{aer}), anaerobic ATP production (ATP_{ana}), and pyrophosphate-associated energy saving (PP_i). Plots therefore present (i) the total energy demand relative to an aerobic reference and (ii) the proportional contribution of each energy source.

All analyses were conducted in Python (version 3.11.13), using NumPy (version 2.3.3) and Pandas (version 2.3.3) for data handling, Matplotlib (version 3.9.1 for visualisation, and the statsmodels (version 0.14.5) for the ANOVA and post hoc testing.

3. Results

3.1. Developmental Gradient of Culm Growth

The discrete phyllochron, the thermal time (ΔTT) required to produce the next leaf [21], increased with developmental stage in all three genotypes, indicating a gradual slowing of leaf appearance from leaf 5 to leaf 15 (Table S1; Figure S1). At leaf 5, KQ228 had the shortest ΔTT (55.9 ± 6.7 °Cd) compared with Q240 (61.3 ± 6.3 °Cd) and SRA3 (63.8 ± 8.9 °Cd). The same rank order held at leaf 10 and leaf 15. Thus, KQ228 consistently produced leaves with less thermal time than Q240 and SRA3, while Q240 and SRA3 did not differ from each other at a given stage (Table S1).

Internode dry mass increased progressively from the youngest to the older internodes within the sampled series (internodes 1 to 12 from the top) in all genotypes (Figure 1A,B). The upper internodes (1 to 5) represented the actively elongating region and exhibited rapid biomass accumulation. Internodes 6 to 10 had largely ceased elongation but continued to accumulate biomass, reflecting ongoing maturation and storage deposition. By internode 12, biomass accumulation had effectively plateaued, indicating fully mature tissue with minimal further gain.

The corresponding rates of biomass accumulation (Figure 1C,D) showed a pronounced peak around internodes 4 to 5. This maximum occurred at, or immediately following, the cessation of elongation, indicating that peak carbon deposition coincides with the transition from structural growth to post-elongation filling. Thereafter, accumulation rates declined sharply across internodes 6 to 12, approaching zero in fully mature tissue.

Genotypic differences were evident in both the magnitude and persistence of biomass accumulation. At mid-season, Q240 and SRA3 exhibited higher peak accumulation rates and a more gradual decline across the internode series, consistent with sustained biomass deposition during maturation. In contrast, KQ228 showed lower peak rates and a more rapid decline, indicating earlier saturation of biomass accumulation.

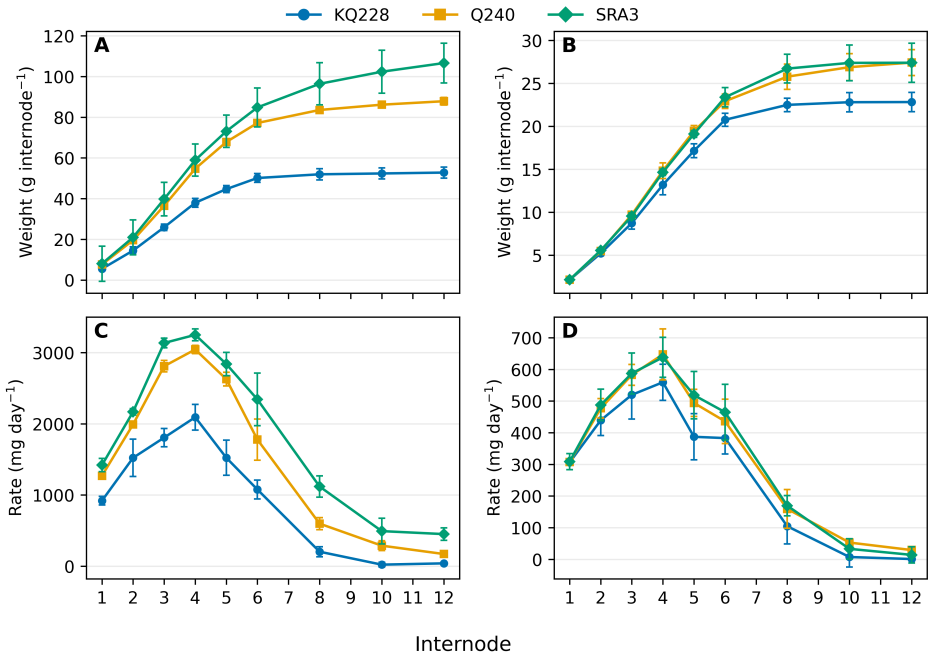


Figure 1. Internode dry biomass (**A**,**B**) and rates of biomass accumulation (**C**,**D**) across the developmental series (internodes 1–12 from the top). Panels (**A**,**B**) represent mid-season (peak growth), while panels (**C**,**D**) represent end-season (maturation). Lines show medians; error bars indicate SD across observations for each genotype.

Internode numbering reflects the relative developmental position along the culm at the time of sampling rather than a fixed anatomical identity. Consequently, internode 12 at mid-season represents a substantially younger and more actively growing tissue than internode 12 at end-season, when overall growth rates are reduced. In developmental terms, internode 12 at mid-season approximately corresponds to a lower-ranked internode (e.g., internodes 26 to 28) later in the season.

The apparent reduction in biomass between mid-season and end-season therefore reflects differences in developmental stage and growth rate at the time of sampling rather than a loss of dry matter.

Together, these patterns define a clear developmental gradient along the culm, in which young internodes function as growth sinks, while older internodes function primarily as storage tissue. Accordingly, the spatial pattern of biomass accumulation (ΔW^{+}) along the internode series establishes the developmental framework for quantifying growth respiration (R_g), maintenance respiration (R_m), and total sink demand.

3.2. Changes in Biomass Composition

Recovery of biomass in the isolated fractions accounted for more than 93% of the total dry weight (Table S2). No significant differences were observed in recovery among genotypes at a given developmental stage. However, within each genotype, recovery efficiency varied across stages of development (Table S3).

Biomass composition varied systematically with internode position (Figure 2). Younger internodes contained a greater proportion of structural material, whereas carbohydrate content increased progressively in older internodes. This compositional transition coincided with the reduction in elongation growth, indicating a shift from structural biomass production to storage-driven accumulation as internodes matured.

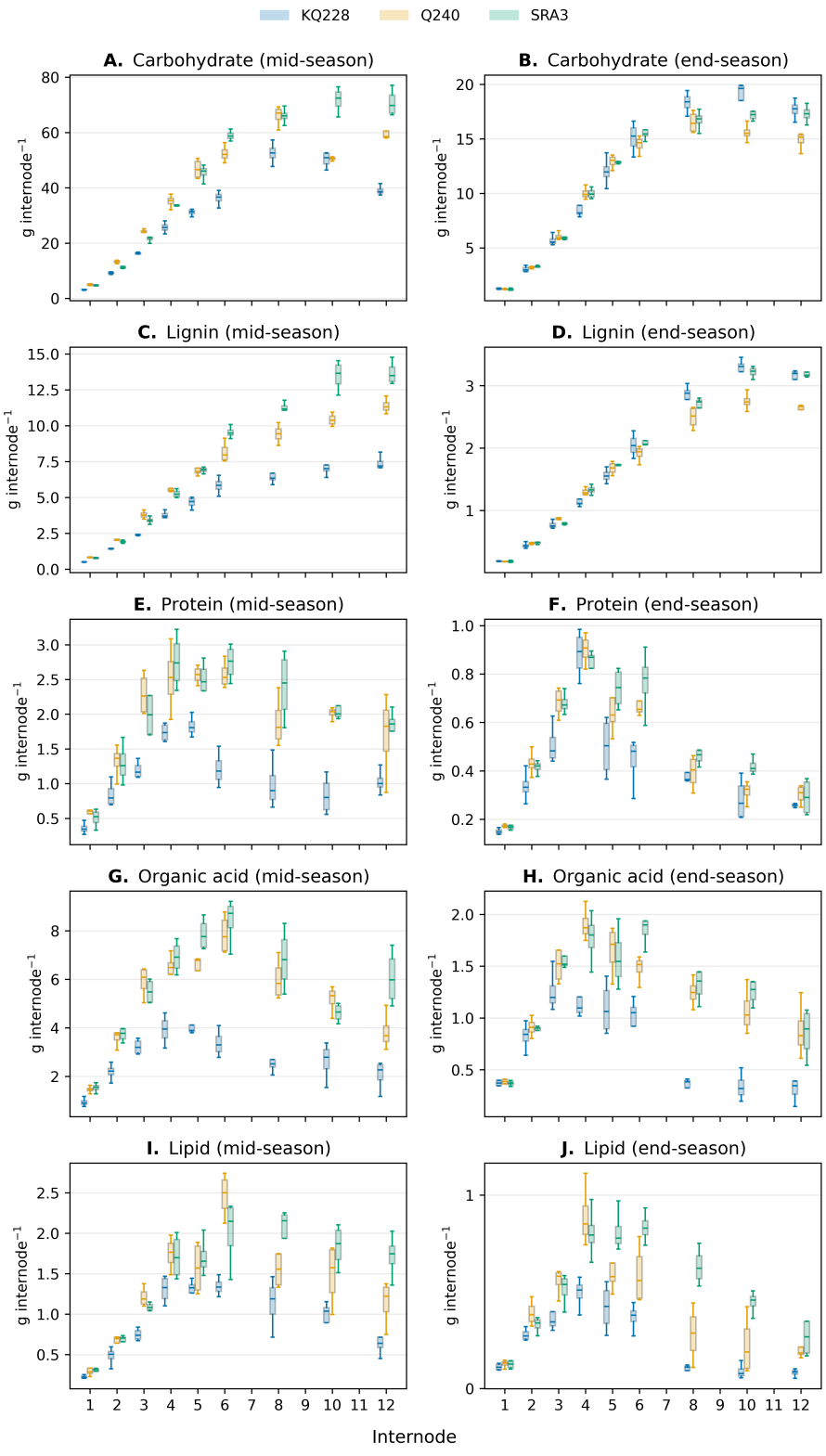


Figure 2. Distribution of major biomass components across internodes in three sugarcane genotypes (KQ228, Q240, SRA3) at contrasting developmental stages. Panels show total carbohydrate (**A**,**B**), lignin (**C**,**D**), protein (**E**,**F**), organic acids (**G**,**H**), and lipid (**I**,**J**) (% dry weight) across internodes (1 to 12) at mid-season (**A**,**C**,**E**,**G**,**I**) and end-season (**B**,**D**,**F**,**H**,**J**). Boxplots represent biological variation among replicates.

Carbohydrates constituted the dominant fraction of internode biomass and increased in close parallel with total dry mass across the developmental gradient (Figure 2A,B; cf.

Figure 1A,B). This pattern was consistent under both mid-season (rapid growth) and end-season (slow growth) conditions, indicating that carbohydrate accumulation is the primary driver of biomass gain. Significant differences were observed among genotypes and between internodes within genotypes (Table S3), with the two fast-growing genotypes exhibiting higher carbohydrate accumulation during peak growth.

Lignin represented the second largest biomass component and increased progressively with internode maturation (Figure 2C,D). Unlike carbohydrates, lignin accumulation showed a more sustained increase across the entire developmental series, reflecting continued cell wall thickening even as elongation slowed. Lignin content was also greater in the fast-growing genotypes during mid-season but converged across genotypes under end-season conditions (Table S4).

In contrast, protein, organic acids, and lipids displayed a transient pattern, peaking in elongating internodes and declining thereafter (Figure 2E–J). These components were most abundant during phases of active growth and metabolic activity but decreased significantly following cessation of elongation (Tables S4–S6), particularly under end-season conditions. This decline reflects a redistribution of carbon away from metabolically active pools toward structural (lignin) and storage (carbohydrate) fractions as internodes transition from growth to maturation.

Collectively, these trends demonstrate a coordinated shift in carbon partitioning during internode development, from metabolically active compounds supporting growth to storage and structural components that dominate mature tissue. This transition underpins the increasing sink strength associated with carbohydrate accumulation while maintaining structural integrity through lignification.

As already evident from the total component levels, there were major shifts in carbon partitioning to the different metabolic components. Between 50 and 80% of carbon was allocated to the carbohydrate pool (Figure S2A,B). The slower the rate of growth, the more reduced carbon was allocated to the carbohydrate pool. There were no significant differences between carbon allocation to the carbohydrate pool between the genotypes during development of the first six internodes in mid-season (Table S8), but there were significant differences during the latter stages of development. Partitioning into carbohydrates varied significantly between young and mature internodes. Partitioning of carbon into lignin increased during internode development but accelerated after cessation of internode expansion (Figure S2C,D and Table S9).

The increased carbon allocation to the carbohydrate pool came at the expense of protein, organic acids, and lipid (Figure S2E–J). The decreased carbon allocation to these three metabolic pools was highly significant, especially after cessation of internode elongation (internode 5) (Tables S10–S12). In the young actively growing internodes, more than 30% of the total reduced carbon was allocated to protein, organic acids, and lipid. This allocation significantly decreased after cessation of internode elongation and during carbohydrate and lignin accumulation (Tables S10–S12).

Cell wall sugar content (Figure S3A,B), as a portion of the total carbohydrate pool, declined progressively from the young to the older internodes at both stages of the cropping cycle, reflecting a transition from structurally active tissues to storage-dominated tissues. This decline was more pronounced at the end of the season, where the overall cell wall content was lower, particularly in the upper internodes.

Sucrose accumulation (Figure S3C,D) showed an inverse pattern, increasing sharply after internode 5. At mid-season, sucrose began to accumulate from approximately internode 5 onward, whereas at end-season, this accumulation was more substantial and extended to higher absolute levels. Genotypic differences were evident, with KQ228 generally exhibiting higher sucrose concentrations in mature internodes than Q240 and SRA3.

Other soluble sugars, dominated by glucose and fructose (Figure S3E,F), displayed a transient peak in intermediate internodes (typically 4 to 5), followed by a marked decline in the older internodes. This pattern was more compressed and lower in magnitude at end-season, suggesting reduced pools of intermediary carbohydrates during maturation.

Across all panels, variability between genotypes was maintained, but the overall developmental trends were conserved, indicating strong positional control over carbon partitioning along the culm.

Detailed component partitioning is shown in Supplementary Figures S2 and S3, but the main pattern was a progressive increase in storage carbohydrates toward mature internodes.

3.3. Growth and Maintenance Respiration

The estimated respiration could be clearly separated into growth and maintenance components (Figure 3). The growth respiration rate (v_{R_g}) (Figure 3A,D) closely tracked the biomass accumulation rate (Figure 1C,D) during mid-season and end-season growth, peaked between internodes 3 and 6, and collapsed during maturation. The maximum R_g values at peak growth (mid-season) occurred in internodes 4 to 6, reaching 750–1280 mg glucose equivalents day^{-1} depending on the genotype. In contrast, the mature internodes (8 to 12) exhibited much lower R_g values, typically below 250 mg glucose equivalents day^{-1} and falling below 100 mg in the oldest internodes.

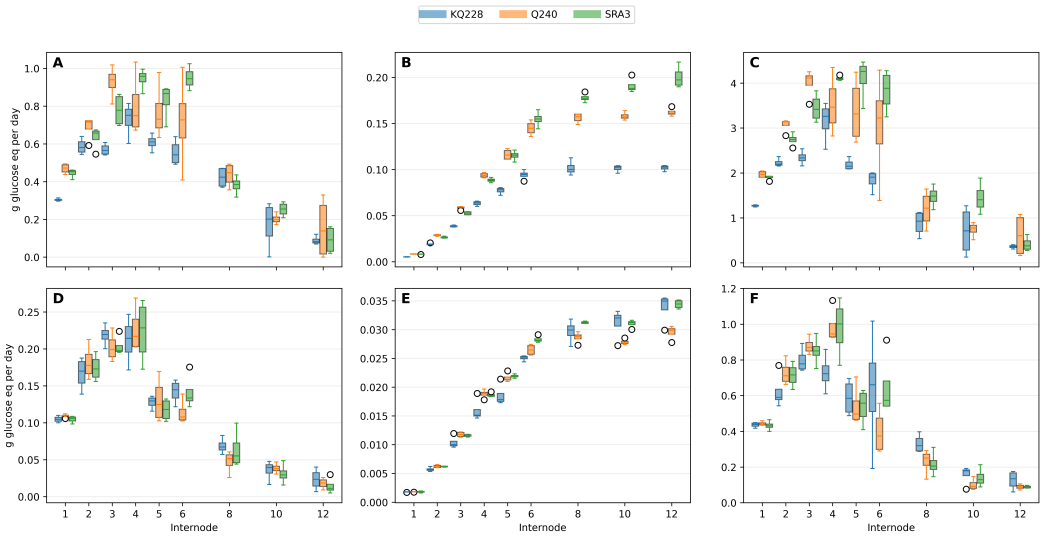


Figure 3. Internode-scale sink demand (glucose equivalents day^{-1}) during mid-season peak growth (**A**–**C**) and end-season slow growth (**D**–**F**). Each panel shows boxplots grouped by genotype (KQ228, Q240, SRA3) across the internodes. The boxes show the interquartile range (IQR) with median lines; whiskers extend to the most extreme non-outlier data; open circles are outliers (Tukey 1.5 IQR rule). (**A**,**D**) Growth respiration rate (v_{R_g}), (**B**,**E**) maintenance respiration rate (v_{R_m}), and (**C**,**F**) total sink demand rate ($v_S = v_{\text{Skel}} + v_{R_g} + v_{R_m}$), where Skel is the carbon skeleton substrate requirement for the observed biomass composition changes.

At the end of the season, growth respiration declined dramatically across the entire culm. In elongating internodes, R_g decreased to approximately 70–230 mg glucose equivalents day^{-1}, and, in mature internodes, it fell below 20 mg glucose equivalents day^{-1}.

Collectively, this demonstrates that (v_{R_g}) is a construction cost and that structural biomass formation was strongly reduced during slow growth at the end of the season.

In contrast, maintenance respiration (v_{R_m}) increased steadily with internode number (i.e., total biomass) (Figure 3B,E). In internode 2, maintenance respiration was only 19–29 mg glucose equivalents day^{-1}, whereas in internode 12, it reached 100–197 mg glucose equivalents day^{-1}. Thus, during peak growth, the elongation zone was dominated

by growth respiration, while mature storage internodes were increasingly dominated by maintenance respiration.

Therefore, mature internodes were not metabolically inactive but rather represented energetically expensive tissue.

Defining "sink strength" for sugarcane stems purely by sucrose concentration, total mass, or organ size neglects the carbon required to build and maintain that biomass. Classical proxies therefore under-estimate true assimilate demand during internode development and ripening. A more faithful measure is to consider both biomass gain and respiratory cost (Supplement S1).

Sink strength (demand) peaked around internodes 4 to 5 (Figure 3C,F). The results demonstrate that a substantial fraction of imported carbon respired to enable biomass accumulation and to sustain the living tissues. Mature storage internodes therefore remain strong sinks even when net structural growth has stopped.

3.4. Sensitivity of Respiratory Demand to Oxygen Limitation

Two hypoxia scenarios were considered by constraining the fraction of ATP demand met by fully aerobic mitochondrial oxidation (oxidative electron transport). In the 0.75 scenario, 75% of the energy demand was met by oxidative phosphorylation, and the remaining 25% was supplied by substrate-level pathways (fermentative metabolism) (Supplement S3. Oxygen-limitation simulations).

These fractions do not represent measured tissue oxygen concentrations. Instead, they approximate physiologically plausible operating states in which oxygen diffusion limits the proportion of ATP that can be generated through oxidative phosphorylation. The scenarios therefore represent energetic constraints on metabolism rather than environmental treatments.

Simulated reductions in mitochondrial energy contribution increased the glucose requirement for respiration across all internodes (Figure 4). The magnitude of the increase was small in rapidly growing internodes but much larger in mature internodes, where maintenance respiration dominated the total demand.

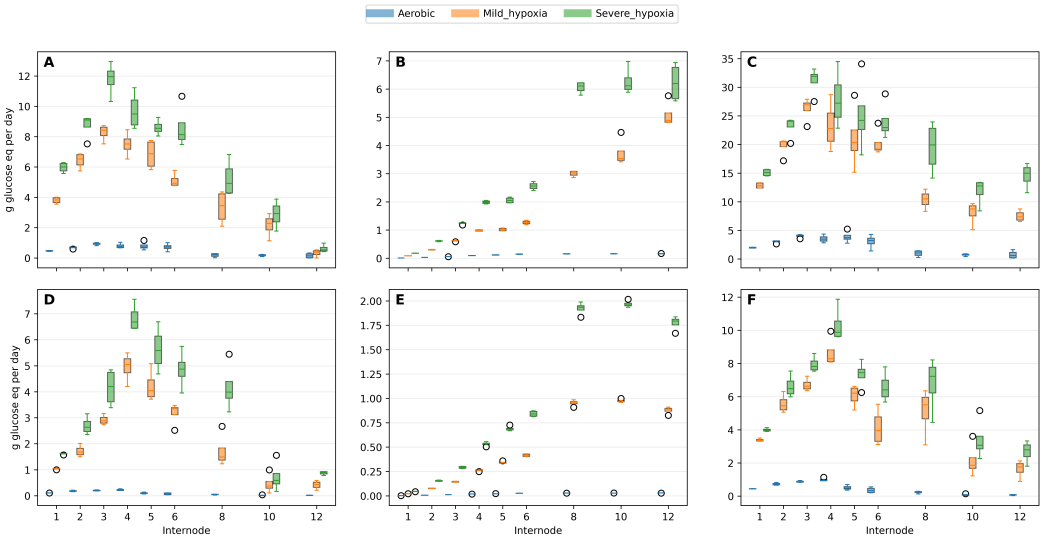


Figure 4. The daily respiratory rates across internodes for three conditions (aerobic, `mild_hypoxia`, `severe_hypoxia`): (**A**,**D**) growth respiration rate (v_{R_g}), (**B**,**E**) maintenance respiration rate (v_{R_m}), and (**C**,**F**) total sink demand rate ($v_S = v_{\text{Skel}} + v_{R_g} + v_{R_m}$), where Skel is the carbon skeleton substrate requirement for the observed biomass composition changes. (**A**–**C**) Mid-season peak growth and (**D**–**F**) end-season slow growth.

The simulations indicate that mature storage tissue is particularly sensitive to reduced oxygen availability because its metabolic demand is largely maintenance-driven rather than growth-driven. Because ATP per glucose falls sharply when a greater share of energy is supplied anaerobically, both R_g (Figure 4A,D) and R_m (Figure 4B,C) require more glucose under hypoxia even when the biomass composition and interval duration are unchanged; the increase is graded (aerobic < mild < severe) at nearly all internodes (Figure 4A–F).

The proportional rise is typically larger for R_m (Figure 4B,E) at later internodes where average supporting mass is higher, so the maintenance share of the sink tends to increase with both stage and hypoxia severity. Because both respiratory components increased total sink, demand is higher under hypoxic conditions.

3.5. Integrated View of Culm Carbon Demand

Combining the developmental gradient with the respiration estimates shows a shift from growth-dominated metabolism to maintenance-dominated metabolism along the culm. Despite reduced structural growth, basal internodes remained metabolically active and continued to require respiratory substrate. A conceptual summary of these relationships is presented in Figure 5.

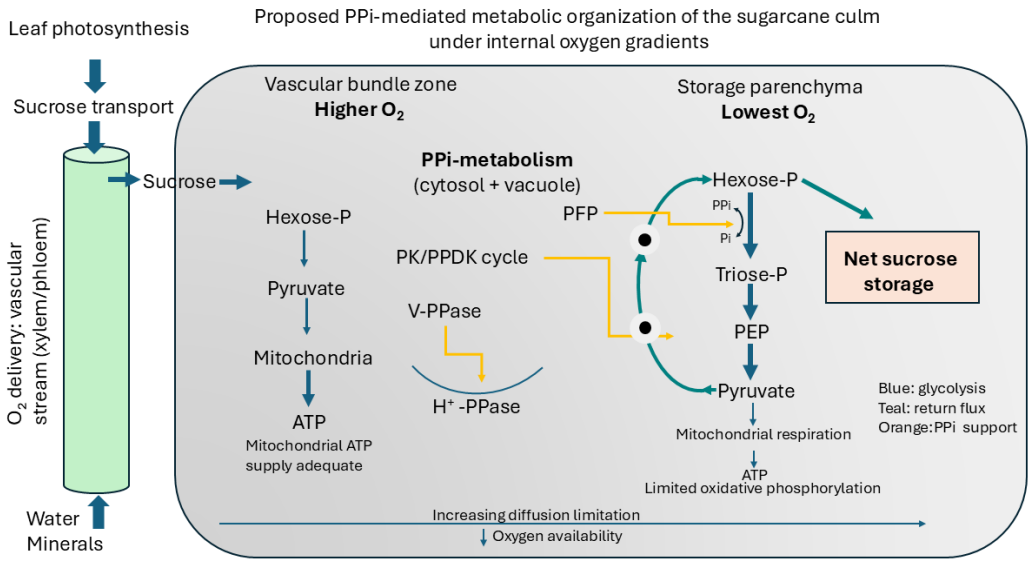


Figure 5. Conceptual model of metabolic organisation in the sugarcane culm under internal oxygen gradients. Sucrose produced by leaf photosynthesis is transported via the vascular system into the culm. Near the vascular bundles, oxygen availability is relatively high, and glycolysis supplies substrates for mitochondrial respiration, supporting the ATP production required for growth metabolism. With increasing distance from the vascular bundles, oxygen diffusion becomes progressively restricted, and storage parenchyma experiences lower oxygen availability. Under these conditions, mitochondrial oxidative phosphorylation becomes constrained, and metabolism increasingly relies on pathways that reduce ATP demand. Pyrophosphate (PPi)-dependent reactions, including pyrophosphate-dependent phosphofructokinase (PFP), the PK/PPDK cycle, and vacuolar H^+-PPase activity, allow metabolic flux to continue with reduced ATP expenditure. This metabolic organisation is consistent with a metabolic configuration that could reduce respiratory carbon loss and facilitates continued sucrose accumulation in mature internodes.

4. Discussion

4.1. Growth and Biomass Accumulation

The spatial pattern of biomass accumulation along the culm reflects a dynamic progression of sink strength rather than a simple sigmoidal growth process. As previously proposed [22], sink strength is determined by the interaction between sink size (internode

volume) and sink activity (metabolic demand), both of which vary systematically along the developmental gradient. Individual internodes therefore represent discrete physiological states, collectively forming a continuum from highly active sinks to mature storage tissues.

Within this framework, sucrose import provides the sole source of carbon to the internode and drives both growth and storage processes. During the elongation phase, strong sink activity is maintained by rapid sucrose turnover through cleavage and resynthesis, ensuring a sustained concentration gradient between the phloem and storage parenchyma. This cycling is coupled to the generation of hexose and hexose–phosphate pools that feed two dominant demand functions: (i) osmolyte accumulation, which is required to sustain turgor and water uptake via vacuolar loading, and (ii) biosynthetic fluxes, which support cell wall formation and cellular metabolism. Together, these processes define the phase of maximal carbon demand and underpin the steep increase in biomass observed in elongating internodes.

The compositional data presented here extend this model by resolving the biochemical fate of the carbon flowing through these pathways. The high abundance of protein, organic acids, and lipids in elongating internodes reflects strong flux through central metabolism, supported by reductant and ATP generation [22]. This metabolically active carbon pool, previously defined as the ROPAL fraction [22], represents the primary sink for carbon during growth and is indicative of high sink activity. Importantly, this phase is also characterised by substantial respiratory demand, as the amount of energy required to sustain these fluxes is considerable.

As internodes transition toward maturity, a fundamental reorganisation of carbon flux occurs. The decline in flux through biosynthetic pathways reduces the demand for hexose utilisation, while continued sucrose import and reduced turnover favour sucrose accumulation in the vacuole. Concurrently, lignification and secondary wall deposition proceed, reflecting the completion of structural development and imposing physical constraints on further expansion. The increasing resistance of the cell wall, associated with rising pressure potential, effectively counteracts the osmotic drive generated by solute accumulation, leading to the cessation of elongation despite high internal sugar concentrations [23–25].

Genotypic differences in biomass accumulation can therefore be interpreted as differences in the temporal regulation of these fluxes. Q240 and SRA3 maintain higher flux through growth-associated pathways across a broader range of internodes, sustaining both osmotic and biosynthetic demand and thereby prolonging the period of active sink function. In contrast, KQ228 exhibits an earlier decline in these fluxes, resulting in reduced sink activity and earlier transition to a storage-dominated state characterised by increased sucrose accumulation and reduced metabolic turnover.

Integration of this flux-based framework with the respiration analysis provides a direct link between carbon partitioning and energy demand. The elongation phase, characterised by high flux, corresponds to the period of maximal growth respiration, where ATP and reductant are required to support biosynthesis and solute accumulation. As flux through these pathways declines, the relative contribution of growth respiration decreases and maintenance respiration becomes dominant, reflecting the reduced metabolic activity of mature tissue. Thus, the transition from elongation to maturation represents not only a shift in carbon allocation but also a rebalancing of the energetic requirements of the tissue.

Collectively, these observations support a unified model in which biomass accumulation is governed by the interaction between sucrose import, its partitioning between storage and metabolic utilisation, and the physical constraints imposed by cell wall development. Internode growth is driven by the coordinated operation of these fluxes, while maturation reflects their progressive uncoupling as structural limitations override osmotic and metabolic drivers of expansion. This framework provides a mechanistic basis

for linking developmental progression, carbon partitioning, and respiratory costs in the sugarcane culm.

Under conditions where ATP supply is constrained, modulation of flux through these pathways—particularly via PPi-dependent reactions [9,12]—may further influence the balance between the storage and metabolic utilisation of sucrose.

4.2. Maintenance Respiration Dominates Mature Storage Tissue

The present results demonstrate a clear developmental transition along the sugarcane culm. Growth respiration dominated in elongating internodes, whereas maintenance respiration became the primary metabolic demand in mature storage tissue. This shift is consistent with general plant carbon balance theory [2,5], but its persistence in a long-lived storage organ is physiologically significant. Mature internodes are not metabolically quiescent; instead, they remain active sinks requiring continuous respiratory substrate despite minimal structural growth.

Sustained sucrose accumulation during maturation therefore depends on the balance between phloem import and the carbon cost of maintenance metabolism. The results show that, although maintenance demand is substantial, net accumulation continues, indicating that respiratory carbon loss does not exceed assimilate supply during ripening.

4.3. Energetic Constraint and Carbon Cost

Simulated reductions in mitochondrial energy contribution increased the glucose requirement for respiration, particularly in mature internodes where maintenance dominates total demand. Under energetic constraint, more substrate is required to generate the same ATP output, increasing the carbon cost of maintaining living tissue. If respiratory efficiency declined substantially, net storage would be expected to decrease.

However, continued sucrose accumulation during maturation suggests that the effective energetic cost of maintenance remains sufficiently low to permit net carbon gain. This indicates that storage parenchyma operates under conditions that preserve respiratory carbon efficiency even when structural growth has largely ceased.

4.4. Distinction Between Measured Data and Model-Derived Interpretation

The experimental component of this study provides direct measurements of biomass accumulation and composition along the culm. In contrast, respiration rates and energetic constraint analyses are derived from these data using a modelling framework.

The simulations are therefore not intended to reproduce exact physiological conditions but rather to evaluate the sensitivity of respiratory carbon demand to reduced energetic efficiency. The conclusions should be interpreted in terms of physiological plausibility and relative responses rather than direct quantification of oxygen limitation within the culm.

4.5. Carbon Conservation and PPi-Supported Metabolic Configuration

Plants subjected to energetic limitation frequently reorganise metabolism to reduce ATP demand [12,26]. In sugarcane and other strong sink tissues, sucrose breakdown via sucrose synthase is coupled to pyrophosphate (PPi) production, providing a potential alternative energy currency. PPi-dependent reactions can partially substitute for ATP-requiring steps, including reactions catalysed by pyrophosphate-dependent phosphofructokinase and vacuolar H^+-PPase.

However, it is important to emphasise that enzyme activities, metabolite levels, and fluxes associated with PPi metabolism were not measured in this study. The proposed role of PPi therefore represents a mechanistic interpretation based on established biochemical principles rather than direct experimental evidence. Alternative mechanisms that reduce ATP demand or improve energetic efficiency may also contribute.

The key finding of this study is therefore not the demonstration of a specific mechanism but rather the identification of a requirement for carbon conservation under maintenance-dominated metabolism in a living storage organ. PPi-dependent reactions can then partially substitute for ATP-requiring steps in cytosolic metabolism, including reactions catalysed by pyrophosphate-dependent phosphofructokinase and vacuolar H^+-PPase [6,14,27]. The developmental pattern observed here—maintenance-dominated metabolism combined with sustained storage—is therefore consistent with a metabolic configuration that limits ATP demand and thereby moderates respiratory carbon loss.

Importantly, this interpretation does not imply cessation of sucrose turnover. Sucrose breakdown continues to support metabolic function, but the carbon cost per unit ATP appears to be constrained. In this framework, the sugarcane culm remains an active and efficient sink throughout maturation.

4.6. Implications for Sucrose Yield

The results indicate that sucrose yield is influenced not only by assimilate supply but also by the respiratory carbon cost of maintaining living storage tissue. Variation in maintenance demand, energetic efficiency, or tolerance to energetic constraint may therefore contribute to genotypic differences in ripening behaviour and storage efficiency. Accounting for variable maintenance respiration during maturation may improve physiological interpretation of yield differences among cultivars.

4.7. Implications for Crop Productivity and Management

These results highlight the respiratory carbon efficiency of the culm as a determinant of sugarcane yield potential. The capacity to conserve carbon during the storage phase may contribute to the unusually high harvest index and sucrose yields achieved by modern cultivars. Genotypic differences in maintenance demand, oxygen limitation tolerance, or propensity to utilise PPi-supported pathways could therefore influence yield and may represent targets for selection.

Environmental conditions that exacerbate internal oxygen limitation (e.g., high soil moisture or waterlogging) may increase the energetic penalty of maintenance metabolism. If PPi-supported metabolism contributes to carbon conservation under such conditions, it may buffer yield loss. Conversely, if the energetic constraint is severe, respiratory carbon costs could increase and reduce storage efficiency. Integrating culm respiration and carbon efficiency into crop models may therefore improve the prediction of sucrose accumulation under contrasting environments.

Sucrose yield in sugarcane depends not only on assimilate supply from photosynthesis but also on the efficiency with which the culm conserves carbon during storage. Because maintenance respiration dominates metabolic demand in mature internodes, respiratory carbon loss represents a potential limitation to final sucrose yield, particularly during the prolonged ripening phase.

If sugarcane culms operate in a low-ATP metabolic state supported partly by PPi-dependent reactions, this mechanism may buffer yield against respiratory losses under energetically constrained conditions. Genotypes that maintain sucrose accumulation despite reduced growth or adverse environmental conditions may therefore do so through improved respiratory carbon efficiency rather than increased photosynthetic supply. This suggests that traits associated with maintenance metabolism, oxygen tolerance, and energy utilisation in the culm could represent useful targets for breeding and physiological phenotyping.

In addition, crop growth models typically represent respiration using fixed coefficients, implicitly assuming constant respiratory efficiency. The present results indicate that respiratory carbon cost varies with developmental stage and oxygen availability. Incorporating variable maintenance respiration and storage efficiency into sugarcane crop models may therefore improve the prediction of sucrose accumulation, particularly during late-season ripening and under wet field conditions.

4.8. Limitations and Interpretation

The present study is based on a modelling framework rather than direct measurements of oxygen concentration, ATP production, or PPi metabolism within the culm. Maintenance respiration is estimated rather than measured directly, and the simulation of oxygen limitation relies on assumed reductions in mitochondrial energy contribution.

Direct measurement of internal oxygen gradients in intact culm tissue is experimentally challenging due to the disruption of diffusion gradients during sampling. Similarly, in-field quantification of metabolites such as PPi is constrained by rapid metabolic changes during tissue excision and processing.

Consequently, the role of PPi-supported metabolism is interpreted as a plausible mechanistic framework consistent with the observed carbon balance rather than as direct experimental evidence. Future studies integrating in situ oxygen measurements, metabolic flux analysis, and enzyme activity profiling will be required to validate these mechanisms.

5. Conclusions

Sugarcane culms exhibit a clear developmental transition from growth-dominated to maintenance-dominated respiration along the internode sequence. Despite increasing maintenance demand in mature internodes, sucrose accumulation continues, indicating that the carbon cost of maintaining living storage tissue remains compatible with sustained net import from the phloem.

Simulated energetic constraints associated with oxygen limitation increase the glucose requirement for respiration, particularly in mature tissue where maintenance costs dominate. However, the continued accumulation of sucrose in these internodes indicates that respiratory carbon efficiency must remain high during maturation.

These results highlight the importance of maintenance metabolism in determining the efficiency of carbon storage in the sugarcane culm. They further suggest that storage tissue may operate in a low-ATP metabolic state in which ATP demand is reduced, potentially through the partial substitution of ATP-dependent reactions with pyrophosphate (PPi)-dependent pathways.

Consequently, sucrose yield potential depends not only on assimilate supply but also on the capacity of culm metabolism to minimise respiratory carbon loss during long-term storage.

Supplementary Materials: The following supporting information can be downloaded at: https://www.mdpi.com/article/10.3390/agronomy16090913/s1: Figure S1: Thermal time vs. phytomer number; Figure S2: Distribution of major biomass components across internodes; Figure S3: Distribution of soluble and structural carbohydrate fractions; Table S1: Carbon mass fractions and construction costs; Table S2: Phyllochron (thermal time differences); Table S3: Lignocellulosic and soluble components (Celignis analysis); Table S4: Biomass recovery across compound classes; Table S5: Carbohydrate content; Table S6: Lignin content; Table S7: Protein content; Table S8: Organic acid content; Table S9: Lipid content; Table S10: Carbohydrate partitioning; Table S11: Lignin partitioning; Table S12: Protein partitioning; Table S13: Organic acid partitioning; Table S14: Lipid partitioning.

Funding: This research was funded by the CRC for Developing Northern Australia, the University of Queensland, and the Queensland Government.

Data Availability Statement: The datasets used and analysed during the current study are available from the corresponding author on request.

Conflicts of Interest: The authors declare no conflicts of interest.

References

1. Moore, P.H. Temporal and Spatial Regulation of Sucrose Accumulation in the Sugarcane Stem. *Funct. Plant Biol.* **1995**, *22*, 661–679. [CrossRef]
2. De Vries, F.P.; Brunsting, A.H.M.; Van Laar, H.H. Products, Requirements and Efficiency of Biosynthesis a Quantitative Approach. *J. Theor. Biol.* **1974**, *45*, 339–377. [CrossRef] [PubMed]
3. De Vries, F.P.; Witlage, J.M.; Kremer, D. Rates of Respiration and of Increase in Structural Dry Matter in Young Wheat, Ryegrass and Maize Plants in Relation to Temperature, to Water Stress and to Their Sugar Content. *Ann. Bot.* **1979**, *44*, 595–609. [CrossRef]
4. De Vries, F.P.; Van Laar, H.; Chardon, M. Bioenergetics of Growth of Seeds, Fruits and Storage Organs. In *Potential Productivity of Field Crops Under Different Environments*; IRRI: Los Baños, Philippines, 1983; pp. 37–60.
5. Amthor, J.S. The McCree–de Wit–Penning de Vries–Thornley Respiration Paradigms: 30 Years Later. *Ann. Bot.* **2000**, *86*, 1–20. [CrossRef]
6. Geigenberger, P. Response of Plant Metabolism to Too Little Oxygen. *Curr. Opin. Plant Biol.* **2003**, *6*, 247–256. [CrossRef]
7. Loreti, E.; Perata, P. The Many Facets of Hypoxia in Plants. *Plants* **2020**, *9*, 745. [CrossRef] [PubMed]
8. Armstrong, W. Aeration in Higher Plants. In *Advances in Botanical Research*; Elsevier: Amsterdam, The Netherlands, 1980; Volume 7, pp. 225–332.
9. Geigenberger, P.; Fernie, A.R.; Gibon, Y.; Christ, M.; Stitt, M. Metabolic Activity Decreases as an Adaptive Response to Low Internal Oxygen in Growing Potato Tubers. *Biol. Chem.* **2000**, *381*, 723–740. [CrossRef] [PubMed]
10. Rolletschek, H.; Radchuk, R.; Klukas, C.; Schreiber, F.; Wobus, U.; Borisjuk, L. Evidence of a Key Role for Photosynthetic Oxygen Release in Oil Storage in Developing Soybean Seeds. *New Phytol.* **2005**, *167*, 777–786. [CrossRef]
11. Rolletschek, H.; Koch, K.; Wobus, U.; Borisjuk, L. Positional Cues for the Starch/Lipid Balance in Maize Kernels and Resource Partitioning to the Embryo. *Plant J.* **2005**, *42*, 69–83. [CrossRef]
12. Igamberdiev, A.U.; Kleczkowski, L.A. Pyrophosphate as an Alternative Energy Currency in Plants. *Biochem. J.* **2021**, *478*, 1515–1524. [CrossRef]
13. Pérez-Castiñeira, J.R.; Docampo, R.; Ezawa, T.; Serrano, A. Pyrophosphates and Polyphosphates in Plants and Microorganisms. *Front. Plant Sci.* **2021**, *12*, 653416. [CrossRef]
14. Stitt, M. Pyrophosphate as an Energy Donor in the Cytosol of Plant Cells: An Enigmatic Alternative to ATP. *Bot. Acta* **1998**, *111*, 167–175. [CrossRef]
15. Bologa, K.L.; Fernie, A.R.; Leisse, A.; Ehlers Loureiro, M.; Geigenberger, P. A Bypass of Sucrose Synthase Leads to Low Internal Oxygen and Impaired Metabolic Performance in Growing Potato Tubers. *Plant Physiol.* **2003**, *132*, 2058–2072. [CrossRef]
16. Mustroph, A.; Hess, N.; Sasidharan, R. Hypoxic Energy Metabolism and PPi as an Alternative Energy Currency. In *Low-Oxygen Stress in Plants: Oxygen Sensing and Adaptive Responses to Hypoxia*; van Dongen, J.T., Licausi, F., Eds.; Springer: Vienna, Austria, 2014; pp. 165–184. [CrossRef]
17. Jeffrey, S.; Carter, J.; Moodie, K.; Beswick, A. Using Spatial Interpolation to Construct a Comprehensive Archive of Australian Climate Data. *Environ. Model. Softw.* **2001**, *16*, 309–330. [CrossRef]
18. Botha, F.C.; Marquardt, A. Metabolic Control of Sugarcane Internode Elongation and Sucrose Accumulation. *Agronomy* **2024**, *14*, 1487. [CrossRef]
19. Dickson, R.E. Analytical Procedures for the Sequential Extraction of 14C-labeled Constituents from Leaves, Bark and Wood of Cottonwood Plants. *Physiol. Plant.* **1979**, *45*, 480–488. [CrossRef]
20. Sun, S.W.; Lin, Y.C.; Weng, Y.M.; Chen, M.J. Efficiency Improvements on Ninhydrin Method for Amino Acid Quantification. *J. Food Compos. Anal.* **2006**, *19*, 112–117. [CrossRef]
21. Wilhelm, W.; McMaster, G.S. Importance of the Phyllochron in Studying Development and Growth in Grasses. *Crop Sci.* **1995**, *35*, 1–3. [CrossRef]
22. Botha, F.C.; Scalia, G.; Marquardt, A.; Wathen-Dunn, K. Sink Strength During Sugarcane Culm Growth: Size Matters. *Sugar Tech* **2023**, *25*, 1047–1060. [CrossRef]
23. Komor, E. Regulation of Futile Cycles: The Transport of Carbon and Nitrogen in Plants. In *Flux Control in Biological Systems*; Schulze, E.D., Ed.; Academic Press: San Diego, CA, USA, 1994; pp. 153–201.
24. Rae, A.; Bonnett, G.; Karno, K. Understanding Stem Development and Sucrose Accumulation to Increase CCS. *Proc. Aust. Soc. Sugarcane Technol.* **2006**, *28*, 2–5.

25. Bottcher, A.; Cesarino, I.; Brombini dos Santos, A.; Vicentini, R.; Mayer, J.; Vanholme, R.; Morreel, K.; Goeminne, G.; Moura, J.C.M.S.; Nobile, P.M.; et al. Lignification in Sugarcane: Biochemical Characterization, Gene Discovery, and Expression Analysis in Two Genotypes Contrasting for Lignin Content. *Plant Physiol.* **2013**, *163*, 1539–1557. [CrossRef]
26. Igamberdiev, A.U.; Kleczkowski, L.A. Magnesium and Cell Energetics in Plants under Anoxia. *Biochem. J.* **2011**, *437*, 373–379. [CrossRef]
27. Plaxton, W.C. The Organization and Regulation of Plant Glycolysis. *Annu. Rev. Plant Biol.* **1996**, *47*, 185–214. [CrossRef]

Disclaimer/Publisher's Note: The statements, opinions and data contained in all publications are solely those of the individual author(s) and contributor(s) and not of MDPI and/or the editor(s). MDPI and/or the editor(s) disclaim responsibility for any injury to people or property resulting from any ideas, methods, instructions or products referred to in the content.